We are IntechOpen, the world's leading publisher of Open Access books Built by scientists, for scientists

6,900
Open access books available

185,000
International authors and editors

200M
Downloads

Our authors are among the

154
Countries delivered to

TOP 1%
most cited scientists

12.2%
Contributors from top 500 universities

WEB OF SCIENCE™

Selection of our books indexed in the Book Citation Index in Web of Science™ Core Collection (BKCI)

Interested in publishing with us?
Contact book.department@intechopen.com

Numbers displayed above are based on latest data collected.
For more information visit www.intechopen.com

15

An Immunological Approach to Mobile Robot Navigation

Guan-Chun Luh and Wei-Wen Liu
Department of Mechanical Engineering, Tatung University
Taiwan, Republic of China

1. Introduction

Autonomous mobile robots have a wide range of applications in industries, hospitals, offices, and even the military, due to their superior mobility. Some of their capabilities include automatic driving, intelligent delivery agents, assistance to the disabled, exploration and map generation for environmental cleanup, etc. In addition, their capabilities also allow them to carry out specialized tasks in environments inaccessible or very hazardous for human beings such as nuclear plants and chemical handling. They are also useful in emergencies for fire extinguishing and rescue operations. Combined with manipulation abilities, their capabilities and efficiency will increase and can be used for dangerous tasks such as security guard, exposition processing, as well as undersea, underground and even space exploration.

In order to adapt the robot's behavior to any complex, varying and unknown environment without further human intervention, intelligent mobile robots should be able to extract information from the environment, use their built-in knowledge to perceive, act and adapt within the environment. An autonomous robot must be able to maneuver effectively in its environment, achieving its goals while avoiding collisions with static and moving obstacles. As a result, motion planning for mobile robots plays an important role in robotics and has thus attracted the attention of researchers recently. The design goal for path planning is to enable a mobile robot to navigate safely and efficiently without collisions to a target position in an unknown and complex environment. The navigation strategies of mobile robots can be generally classified into two categories, global path planning and local reactive navigation. The former is done offline and the robot has complete prior knowledge about the shape, location, orientation, and even the movements of the obstacles in the environment. Its path is derived utilizing some optimization techniques to minimize the cost of the search. However, it has difficulty handling a modification of the environment, due to some uncertain environmental situations, and the reactive navigation capabilities are indispensable since the real-world environments are apt to change over time. On the other hand, local reactive navigation employing some reactive strategies to perceive the environment based on the sensory information and path planning is done online. The robot has to acquire a set of stimulus-action mechanisms through its sensory inputs, such as distance information from sonar and laser sensors, visual information from cameras or processed data derived after appropriate fusion of numerous sensor outputs. The action

taken by the robot is usually an alternation of steering angle and/or translation velocity to avoid collisions and reach the desired target. Nevertheless, it does not guarantee a solution for the mission, nor is the solution the optimal one.

Reactive behavior-based mobile robot responds to stimuli from the dynamic environment, and its behaviors are guided by local states of the world. Its behavior representation is situated at a sub-symbolic level that is integrated into its perception-action (*i.e.*, sensor-motor) capacities analogous to the manifestation of the reflex behavior observed in biological systems. Some researches have focused on this kind of robot system and have demonstrated its robustness and flexibility against an unstructured world (Chang, 1996). Reactive behavior-based strategy is now becoming attractive in the field of mobile robotics (Lee, et al., 1997) to teach the robot to reach the goal and avoid obstacles. Two different kind of reactive navigation strategies have been studied. The first application task for the mobile robot is to navigate in a stationary environment while avoiding static obstacles but reaching a goal safely. A well-known drawback is that the mobile robot suffers from local minima problems in that it uses only locally available environmental information without any previous memory. In other words, a robot may get trapped in front of an obstacle or wander indefinitely in a region whenever it navigates past obstacles toward a target position. This happens particularly if the environment consists of concave obstacles, mazes, etc. Several trap escape algorithms, including the random walk method (Baraquand and Latombe, 1990), the multi-potential field method (Chang, 1996), the tangent algorithm (Lee, et al., 1997), the wall-following method (Yun and Tan, 1997), the virtual obstacle scheme (Liu et al., 2000), and the virtual target approach (Xu, 2000) have been proposed to solve the local minima problems. The second application task is to navigate mobile robot in an unknown and dynamic environment while avoiding moving obstacles. Various methods have been proposed for this purpose, such as configuration-time space based method (Fujimura and Samet, 1989), planning in space and time independently (Ferrari et al., 1998), cooperative collision avoidance and navigation (Fujimori, 2005), fuzzy based method (Mucientes et al., 2001), velocity obstacles method (Prassler et al., 2001), collision cone approach (Qu et al., 2004), and potential field method (Ge and Cui, 1989). Another approach for motion planning of mobile robots is the Velocity Obstacle (VO) method first proposed by Fiorini and Shiller (Fiorini and Shiller, 1998).

In the last decade, it has been shown that the biologically inspired artificial immune system (AIS) has a great potential in the fields of machine learning, computer science and engineering (Castro and Jonathan, 1999). Dasgupta (1999) summarized that the immune system has the following features: self-organizing, memory, recognition, adaptation, and learning. The concepts of the artificial immune system are inspired by ideas, processes, and components, which extracted from the biological immune system. A growing number of researches investigate the interactions between various components of the immune system or the overall behaviors of the systems based on an immunological point of view. Immunized systems consisting of agents (immune-related cells) may have adaptation and learning capabilities similar to artificial neural networks, except that they are based on dynamic cooperation of agents (Ishida, 1997). Moreover, immune systems provide an excellent model of adaptive process operating at the local level and of useful behavior emerging at the global level (Luh and Cheng, 2002). Accordingly, the artificial immune system can be expected to provide various feasible ideas for the applications of mobile robots (Ishiguro et al., 1997; Lee and Sim, 1997; Hart et al., 2003; Duan et al., 2005). As to

mobile robot navigation problem, Ishiguro *et al.* (1995) proposed a two-layer (situation-oriented and goal-oriented) immune network to behavior control of autonomous mobile robots. Simulation results show that mobile robot can reach goal without colliding fixed or moving obstacles. Later, Lee *et al*. (2000) constructed obstacle-avoidance and goal-approach immune networks for the same purpose. Additionally, it shows the advantage of not falling into a local loop. Afterward, Vargas *et al.* (2003) developed an Immuno-Genetic Network for autonomous navigation. The simulations show that the evolved immune network is capable of correctly coordinating the system towards the objective of the navigation task. In addition, some preliminary experiment on a real Khepera II robot demonstrated the feasibility of the network. Recently, Duan et al. (2004) proposed an immune algorithm for path planning of a car-like wheeled mobile robot. Simulations indicate that the algorithm can finish different tasks within shorter time. It should be noted that, however, all of the above researches did not consider solving the local minima problems. Besides, none relative researches implement AIS for mobile robot navigating in dynamic environments.

Two different kind of reactive immune networks inspired by the biological immune system for robot navigation (goal-reaching and obstacle-avoidance) are constructed in this study. The first one is a potential filed based immune network with an adaptive virtual target mechanism to solve the local minima problem navigating in stationary environments. Simulation and experimental results show that the mobile robot is capable of avoiding stationary obstacles, escaping traps, and reaching the goal efficiently and effectively. Employing the Velocity Obstacle method to determine the imminent collision obstacle, the second architecture guide the robot avoiding collision with the most danger object (moving obstacle) at every time instant. Simulation and experimental results are presented to verify the effectiveness of the proposed architecture in dynamic environment.

2. Biological immune system

The immune system protects living organisms from foreign substances such as viruses, bacteria, and other parasites (called antigens). The body identifies invading antigens through two inter-related systems: the innate immune system and the adaptive immune system. A major difference between these two systems is that adaptive cells are more antigen-specific and have greater memory capacity than innate cells. Both systems depend upon the activity of white blood cells where the innate immunity is mediated mainly by phagocytes, and the adaptive immunity is mediated by lymphocytes as summarized in Fig. 1. The phagocytes possess the capability of ingesting and digesting several microorganisms and antigenic particles on contact. The adaptive immune system uses lymphocytes that can quickly change in order to destroy antigens that have entered the bloodstream. Lymphocytes are responsible for the recognition and elimination of the antigens. They usually become active when there is some kind of interaction with an antigenic stimulus leading to the activation and proliferation of the lymphocytes. Two main types of lymphocytes, namely B-cells and T-cells, play a remarkable role in both immunities [34]. Both B-cell and T-cell express in their surfaces antigenic receptors highly specific to a given antigenic determinant. The former takes part in the humoral immunity and secrete antibodies by the clonal proliferation while the latter takes part in cell-mediated immunity. One class of the T-cells, called the Killer T-cells, destroys the infected cell whenever it recognizes the infection. The other class that triggers clonal expansion and stimulates or suppresses antibody formation is called the Helper T-cells.

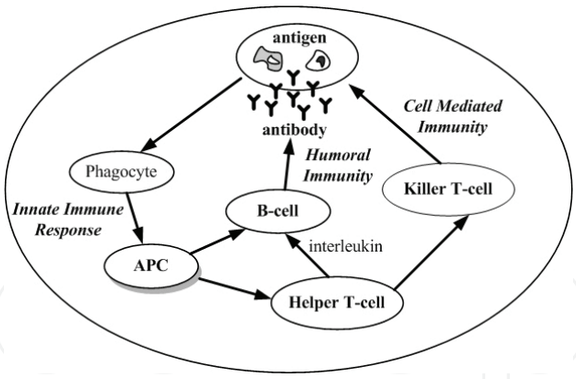

Figure 1 Illustration of the biological immune system

When an infectious foreign pathogen attacks the human body, the innate immune system is activated as the first line of defense. Innate immunity is not directed in any way towards specific invaders but against any pathogens that enter the body. It is called the non-specific immune response. The most important cell in innate immunity is a phagocyte, which internalizes and destroys the invaders to the human body. Then the phagocyte becomes an Antigen Presenting Cell (APC). The APC interprets the antigen appendage and extracts the features by processing and presenting antigenic peptides on its surface to the T-cells and B-cells. These lymphocytes will be able to sensitize this antigen and be activated. Then the Helper T-cell releases the cytokines that are the proliferative signals acting on the producing B-cell or remote the other cells. On the other hand, the B-cell becomes stimulated and creates antibodies when it recognizes an antigen. Recognition is achieved by inter-cellular binding, which is determined by molecular shape and electrostatic charge. The secreted antibodies are the soluble receptor of B-cells and these antibodies can be distributed throughout the body (Oprea, 1996). An antibody's paratope can bind an antigen's epitope according to its affinity. Moreover, B-cells are also affected by Helper T-cells during the immune responses (Carneiro et al., 1996). The Helper T-cell plays a remarkable key role for deciding if the immune system uses cell-mediated immunity or humoral immunity (Roitt et al. 1998), and it connects the non-specific immune response to make a more efficient specific immune response. The Helper-T cells work primarily by secreting substances known as cytokines and their relatives (Roitt et al. 1998) that constitute powerful chemical messengers. In addition to promoting cellular growth, activation and regulation, cytokines can also kill target cells and stimulated macrophages.

The immune system produces the diverse antibodies by recognizing the idiotype of the mutual receptors of the antigens between antigen and antibodies and between antibodies. The relation between antigens and antibodies and that amongst antibodies can be evaluated by the value of the affinity. In terms of affinities, the immune system self-regulates the production of antibodies and diverse antibodies. Affinity maturation occurs when the maturation rate of a B-cell clone increases in response to a match between the clone's antibody and an antigen. Those mutant cells are bound more tightly and stimulated to divide more rapidly. Affinity maturation dynamically balances exploration versus exploitation in adaptive immunity (Dasgupta, 1997). It has been demonstrated that the immune system has the capability to recognize foreign pathogens, learn and memorize, process information, and discriminate between self and non-self. In addition, the system can be maintained even faced with a dynamically changing environment.

Jerne (1973) has proposed the idiotypic network hypothesis (immune network hypothesis) based on mutual stimulation and suppression between antibodies as Fig. 2 illustrates. This hypothesis is modeled as a differential equation simulating the concentration of a set of lymphocytes. The concept of an immune network states that the network dynamically maintains the memory using feedback mechanisms within the network. The various species of lymphocytes are not isolated but communicate with each other through the interaction antibodies. Jerne concluded that the immune system is similar to the nervous system when viewed as a functional network. Based on his speculation, several theories and mathematical models have been proposed (Farmer et al., 1986; Hoffmann, 1989; Carneiro et al., 1996). In this study, the dynamic equation proposed by Farmer (1986) is employed as a reactive immune network to calculate the variation on the concentration of antibodies, as shown in the following equations:

$$\frac{dA_i(t)}{dt} = \left(\sum_{\ell=1}^{N_{Ab}} m_{i\ell}^{st} a_\ell(t) - \sum_{k=1}^{N_{Ab}} m_{ki}^{su} a_k(t) + m_i - k_i \right) a_i(t) \tag{1}$$

$$a_i(t) = \frac{1}{1 + \exp(0.5 - A_i(t))} \tag{2}$$

where i, ℓ, k = 0, 1,$\cdots$, N_{Ab} are the subscripts to distinguish the antibody types and N_{Ab} is the number of antibodies. A_i and a_i are the stimulus and concentration of the ith antibody. m_{ij}^{st}, m_{ki}^{su} indicate the stimulative and suppressive affinity between the ith and the jth, kth antibodies, respectively. m_i denotes the affinity of antigen and antibody i, and k_i represents the natural death coefficient. Equation (1) is composed of four terms. The first term shows the stimulation, while the second term depicts the suppressive interaction between the antibodies. The third term is the stimulus from the antigen, and the final term is the natural extinction term, which indicates the dissipation tendency in the absence of any interaction. Equation (2) is a squashing function to ensure the stability of the concentration (Ishiguro et al., 1997).

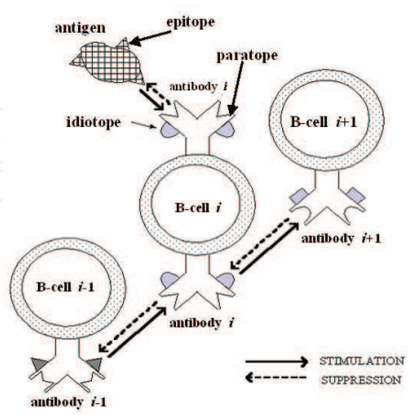

Figure 2. Idiotypic network hypothesis

On the other hand, Hightower *et al.* (1995) suggested that all possible antigens could be declared as a group of set points in an antigen space and antigen molecules with similar shapes occupy neighboring points in that space. It indicates that an antibody molecule can

recognize some set of antigens and consequently covers some portion of antigen space as Fig. 3 illustrated. The collective immune response of the immune network is represented as $\sum_{i=1}^{N_{Ab}} f(Ab_i)$, where $f(Ab_i)$ indicates the immune response function between antigen and the ith antibody. Note that any antigen in the overlapping converge could be recognized by several different antibodies simultaneously. Afterward, Timmis *et al*. (1999) introduced similar concept named Artificial Recognition Ball (ARB). Each ARB represents a certain number of B-cells or resources, and total number of resources of system is limited. In addition, each ARB describes a multi-dimensional data item that could be matched to an antigen or to another ARB in the network by Euclidean distance. Those ARBs located in the other's influence regions would either be merged to limit the population growth or pulled away to explore new area. ARBs are essentially a compression mechanism that takes the B-cells to a higher granularity level.

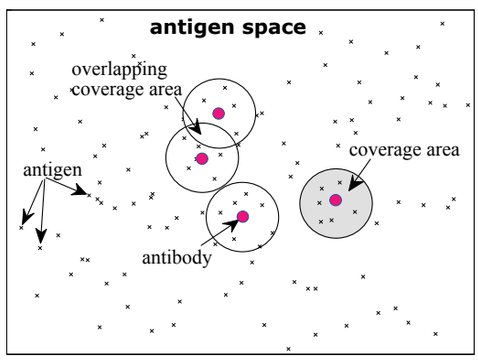

Figure 3. The antigen space

3. Motion Planning in Stationary Environments

3.1 Reactive immune network

A reactive immune network inspired by the biological immune system for robot navigation (goal-reaching and obstacle-avoidance) in stationary environments is described in this section. The architecture of the proposed navigation system is depicted in Fig. 4. The antigen's epitope is a situation detected by sensors and provides the information about the relationship between the current location and the obstacles, along with the target. This scene-based spatial relationship is consistently discriminative between different parts of an environment, and the same representation can be used for different environments. Therefore, this method is tolerant with respect to the environmental changes. The interpreter is regarded as a phagocyte and translates sensor data into perception. The antigen presentation proceeds from the information extraction to the perception translation. An antigen may have several different epitopes, which means that an antigen can be recognized by a number of different antibodies. However, an antibody can bind only one antigen's epitope. In the proposed mechanism, a paratope with a built-in robot's steering direction is regarded as a antibody and interacts with each other and with its environment. These antibodies/steering-directions are induced by recognition of the available antigens/detected-information. In should be noted that only one antibody with the highest concentration will be selected to act according to the immune network hypothesis.

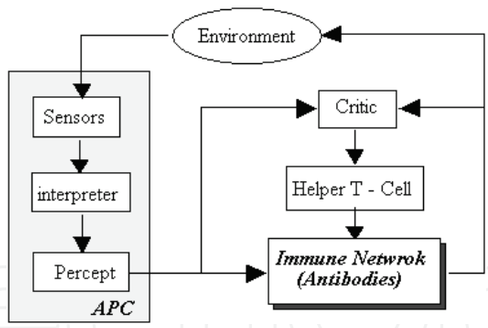

Figure 4. The architecture of the immunized network reactive system

In the proposed immune network, antibodies are defined as the steering directions of mobile robots as illustrated in Fig. 5,

$$Ab_i \equiv \theta_i = \frac{360°}{N_{Ab}}(i-1) \qquad i = 1,2,\cdots,N_{Ab}\ ,$$

where N_{Ab} is the number of antibodies/steering-directions and θ_i is the steering angle between the moving path and the head orientation of the mobile robot. Note that $0° \leq \theta_i \leq 360°$.

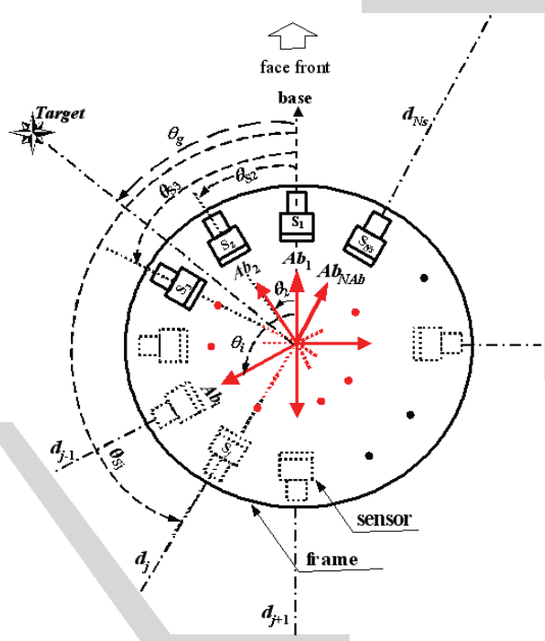

Figure 5. Configuration of mobile robot and its relatives to target and obstacles

In addition, the antigen represents the local environment surrounding the robot and its epitopes are a fusion data set containing the azimuth of the goal position θ_g, the distance between the obstacles and the *jth* sensor d_j, and the azimuth of sensor θ_{Sj},

$$\theta_{S_j} \equiv \frac{360°}{N_S}(j-1) \qquad j = 1,2,\cdots,N_s\,,$$

$$Ag_j \equiv \{\theta_g, d_j, \theta_{S_j}\} \qquad j = 1,2,\cdots,N_s$$

where N_s is the number of sensors equally spaced around the base plate of the mobile robot, $d_{\min} \leq d_j \leq d_{\max}$ and $0° \leq \theta_{S_j} \leq 360°$. Parameters $d_{\min}$ and $d_{\max}$ represent the nearest and longest distances measured by the range sensors, respectively. It should be noted that different antigens (local environments) might have identical epitopes (fusion information from range sensors). There is no necessary relationship between N_{Ab} and N_s since they depend on the hardware (*i.e.* motor steering angles and number of sensors installed) of mobile robot. Nevertheless, simulation results show that better performance could be derived if N_s equal to or larger than N_{Ab}.

The potential-field method is one of the most popular approaches employed to navigate the mobile robot within environments containing obstacles, since it is conceptually effective and easy to implement. The method can be implemented either for off-line global planning if the environment is previously known or for real-time local navigation in an unknown environment using onboard sensors. The Artificial Potential Field (APF) approach considers a virtual attractive force between the robot and the target as well as virtual repulsive forces between the robot and the obstacles. The resultant force on the robot is then used to decide the direction of its movements. In the proposed immune network, the resultant force on the robot is defined as m_i, the affinity value between the antigen/local environment and the *ith* antibody/steering angle,

$$m_i = w_1 F_{goal_i} + w_2 F_{obs_i} \qquad i = 1,2,\cdots,N_{Ab} \tag{3}$$

The weighing values w_1 and w_2 indicate the ratio between attractive and repulsive forces. Note that $0 \leq w_1, w_2 \leq 1$ and $w_1 + w_2 = 1$. The attractive force F_{goal_i} of the ith steering direction (*i.e.* the ith antibody) is defined as follows:

$$F_{goal_i} = \frac{1.0 + \cos(\theta_i - \theta_g)}{2.0}, \qquad i = 1,2,\cdots,N_{Ab} \tag{4}$$

Note that F_{goal_i} is normalized and $0 \leq F_{goal_i} \leq 1$. Obviously, the attractive force is at its maximal level ($F_{goal_i}=1$) when the mobile robot goes straightforward to the target (*i.e.* $\theta_i = \theta_g$). On the contrary, it is minimized ($F_{goal_i}=0$) if the robot's steering direction is the opposite of the goal.

The repulsive force for each moving direction (the ith antibody θ_i) is expressed as the following equation,

$$F_{obs_i} = \sum_{j=1}^{N_S} \alpha_{ij} \cdot \bar{d}_j \tag{5}$$

where $a_{ij} = \exp(-N_s \times (1-\delta_{ij}))$ with $\delta_{ij} = [1+\cos(\theta_i - \theta_{S_j})]/2$. Fig. 6 demonstrates the relationship between α_{ij} and δ_{ij}. The parameter α_{ij} indicates the weighting ratio for the jth sensor to steering angle θ_i while $\bar{d}_j$ represents the normalized distance between the jth sensor and the

obstacles. Coefficient δ_{ij} expresses influence and importance of each sensor at different locations. The equation shows that the information derived from the sensor closest to the steering direction is much more important due to its biggest δ_{ij} value. Kubota *et al.* (2001) have proposed a similar 'delta rule' to evaluate the weighting of each sensor too.

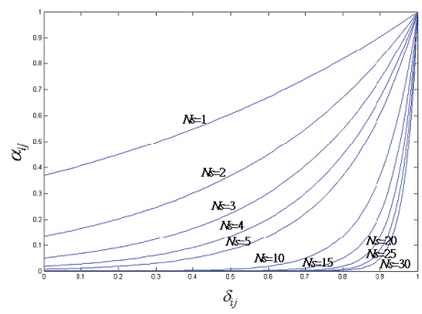

Figure 6. Relation between α_{ij} and δ_{ij}

The normalized obstacle distance for each sensor $\overline{d}_j$ is fuzzified using the fuzzy set definitions. The mapping from the fuzzy subspace to the TSK model is represented as three fuzzy if-then rules in the form of

$$\begin{array}{llll} \text{IF} & d_j \text{ is } \mathbf{s} & \text{THEN} & \text{y} = L_1 \\ \text{IF} & d_j \text{ is } \mathbf{m} & \text{THEN} & \text{y} = L_2 \\ \text{IF} & d_j \text{ is } \mathbf{d} & \text{THEN} & \text{y} = L_3 \end{array}$$

where L_1, L_2, and L_3 are defined as 0.25, 0.5 and 1.0, respectively. The input variable of each rule is the detected distance d_j of the jth sensor. The antecedent part of each rule has one of the three labels, namely, **s** (safe), **m** (medium), and **d** (danger). Consequently, the total output of the fuzzy model is given by the equation below,

$$\overline{d}_j = \frac{\mu_{safe}(d) \cdot L_1 + \mu_{medium}(d) \cdot L_2 + \mu_{danger}(d) \cdot L_3}{\mu_{safe}(d) + \mu_{medium}(d) + \mu_{danger}(d)} \tag{6}$$

where $\mu_{safe}(d)$, $\mu_{medium}(d)$, $\mu_{danger}(d)$ represent the matching degree of the corresponding rule. Fig. 7 illustrates the membership function and labels for measured distance d_j.

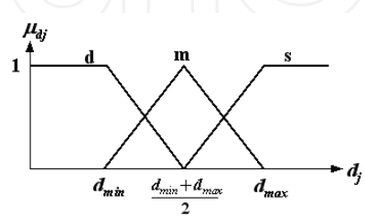

Figure 7. Membership function and labels for measured distance d_j

As to the stimulative-suppressive interaction between the antibodies/steering-directions are derived from equation (1) as follows,

$$\begin{aligned}
\frac{dA_i(t)}{dt} &= \left(\sum_{\ell=1}^{N_{Ab}} m_{i\ell}^{st} a_\ell(t) - \sum_{k=1}^{N_{Ab}} m_{ki}^{su} a_k(t) + m_i - k_i \right) a_i(t) \\
&= \left[\left(m_{i1}^{st} a_1(t) + m_{i2}^{st} a_2(t) + \cdots + m_{iN_{Ab}}^{st} a_{N_{Ab}}(t) \right) - \left(m_{1i}^{su} a_1(t) + m_{2i}^{su} a_2(t) + \cdots + m_{N_{Ab}i}^{su} a_{N_{Ab}}(t) \right) + m_i - k_i \right] a_i(t) \\
&= \left[\left(m_{i1}^{st} - m_{1i}^{su} \right) a_1(t) + \left(m_{i2}^{st} - m_{2i}^{su} \right) a_2(t) + \cdots + \left(m_{iN_{Ab}}^{st} - m_{N_{Ab}i}^{su} \right) a_{N_{Ab}}(t) + m_i - k_i \right] a_i(t) \\
&= \left[m_{i1}^{ss} a_1(t) + m_{i2}^{ss} a_2(t) + \cdots + m_{iN_{Ab}}^{ss} a_{N_{Ab}}(t) + m_i - k_i \right] a_i(t) \\
&= \left(\sum_{\ell=1}^{N_{Ab}} m_{i\ell}^{ss} a_\ell(t) + m_i - k_i \right) a_i(t)
\end{aligned}$$

and the stimulative-suppressive affinity $m_{i\ell}^{ss}$ between the ith and jth antibody/steering-angle is defined as

$$m_{i\ell}^{ss} = m_{i\ell}^{st} - m_{\ell i}^{su} = \cos(\theta_i - \theta_\ell) = \cos(\Delta\theta_{i\ell}), \quad i, \ell = 1,2,\cdots,N_{Ab} \tag{7}$$

Obviously, stimulative-suppressive effect is positive ($m_{i\ell}^{ss}$ >0) if $-90° < \Delta\theta_{i\ell} < 90°$. On the contrary, negative stimulative-suppressive effect exists between two antibodies if their difference of steering angles are greater than 90° or less than -90° (*i.e.*, $\Delta\theta_{i\ell} > 90°$ or $\Delta\theta_{i\ell} < -90°$). In addition, there is no any net effect between orthogonal antibodies (*i.e.* $\Delta\theta_{i\ell} = \pm 90°$). The immune system responses to the specified winning situation that has the maximum concentration among the trigged antibodies by comparing the currently perceived situations (trigged antibodies). In other words, antibody with the highest concentration is selected to activate its corresponding behavior to the world. Therefore, mobile robot moves a step along the direction of the chosen steering angle/antibody.

3.2 Local minimum recovery

As mentioned in the previous section, one problem inherent in the APF method is the possibility for the robot to get trapped in a local minima situation. Traps can be created by a variety of obstacle configurations. The key issue to the local minima problems is the detection of the local minima situation during the robot's traversal. In this study, the comparison between the robot-to-target direction θ_g and the actual instantaneous direction of travel θ_i was utilized to detect if the robot got trapped. The robot is very likely to get trapped and starts to move away from the goal if the robot's direction of travel is more than 90°off-target (*i.e.* $|\theta_i - \theta_g|$>90°). Various approaches for escaping trapping situations have been proposed as described previously. In this study, an adaptive virtual target method is developed and integrated with the reactive immune network to guide the robot out of the trap.

In immunology, the T-cell plays a remarkable key role in distinguishing a "self" from other "non-self" antigens. The Helper-T cells work primarily by secreting substances to constitute powerful chemical messengers to promote cellular growth, activation and regulation. Simulating the biological immune system, this material can either stimulate or suppress the promotion of antibodies/steering-directions depending on whether the antigen is non-self or self (trapped in local minima or not). Different from the virtual target method proposed in [10-11], an additional virtual robot-to-target angle θ_v (analogous to the interleukine secreted by T-cells) is added to the goal angle θ_g whenever the trap condition ($|\theta_i - \theta_g|$>90°) is satisfied,

$$\theta_g(k+1) = \theta_g(k) + \theta_v(k) \tag{8}$$

with

$$\begin{cases} \theta_v(k) = \theta_v(k-1) \pm \Delta\theta_g & \text{if } \left|\theta_i(k) - \theta_g(k)\right| \geq 90^\circ \text{ and } \theta_v(k-1) = 0 \\ \theta_v(k) = \theta_v(k-1) + sign\left(\theta_v(k-1)\right) \cdot \Delta\theta_g & \text{if } \left|\theta_i(k) - \theta_g(k)\right| \geq 90^\circ \text{ and } \theta_v(k-1) \neq 0 \\ \theta_v(k) = \max\left\{0, \theta_v(k-1) - sign\left(\theta_v(k-1)\right) \cdot \theta_c(k-1)\right\} & \text{if } \left|\theta_i(k) - \theta_g(k)\right| < 90^\circ \text{ and } \theta_v(k-1) \geq 0 \\ \theta_v(k) = \min\left\{0, \theta_v(k-1) - sign\left(\theta_v(k-1)\right) \cdot \theta_c(k-1)\right\} & \text{if } \left|\theta_i(k) - \theta_g(k)\right| < 90^\circ \text{ and } \theta_v(k-1) < 0 \end{cases}$$

where $\Delta\theta_g = \theta_g(k) - \theta_g(k-1)$ and $\theta_c(k) = \theta_c(k-1) + \lambda$.

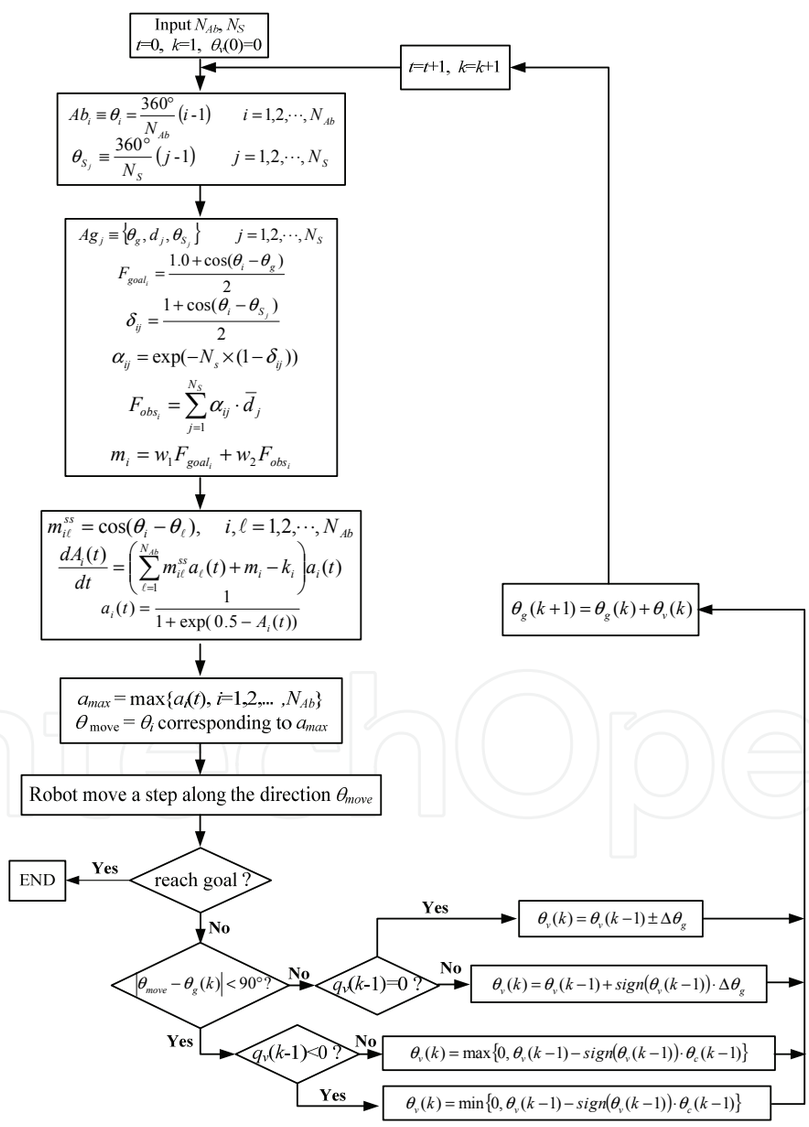

Figure 8. Flowchart of the mobile robot navigation procedure

Parameters k-1, k, and k+1 represent the previous state, the current state and the future state, respectively. Symbol "±" indicates that the location of the virtual target can be randomly switched to either the right (*i.e.* "+") or the left (*i.e.* "−") side of the mobile robot so that the robot has a higher probability of escaping from the local minima in either direction. λ is an adjustable decay angle. The bigger the value is, the faster the location of virtual target converges to that of the true one and the easier it is for the robot to get trapped in the local minima again. In this study, λ is determined after multiple simulation runs and set to 0.2. The incremental virtual angle $\theta_v(k)$ in the proposed scheme is state dependent and self-adjustable according to the robot's current state and the action it took previously. This provides powerful and effective trap-escaping capability compared to virtual target method, which keeps θ_v a constant value. θ_c is a converging angle and its initial value is 0. Fig. 8 shows the flowchart of navigation procedure for mobile robot employing the proposed reactive immune network.

For carrying out the necessary simulation and validating the efficacy of the proposed methodology, a computer program was developed using C++ language with graphical user interface. The simulation environment contains a robot and obstacle constructed by numerous square blocks 10cm in length. The environmental condition adopted in simulation is a 300cm×300cm grid. The size of the simulated robot is a circle with 10cm diameter. During each excursion, the robot tries to reach target and avoid collision with obstacle. Fig. 9 elucidates and demonstrates the performance of the proposed strategy for the robot to escape from a recursive U-trap situation, which may make the virtual target switching strategy (Xu, 2000) ineffective as Chatterjee and Matsuno (2001) suggested.

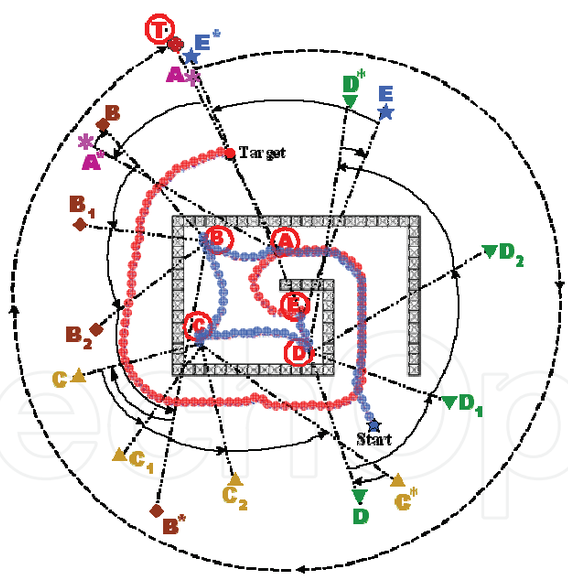

Figure 9. Robot path and state of the indices along the trajectory

The robot first enters a U-shaped obstacle and is attracted to the target due to the target's reaching behavior until it reaches the critical point Ⓐ. Clearly, the azimuth of goal θ_g is kept the same during this stage; however, the distance between the robot and the target is decreased quickly. The detection of the trap possibility because of the abrupt change of target orientation at location Ⓐ (θ_g) makes the target shift to a virtual position A* (θ_g - $\Delta\theta_g$).

$\Delta\theta_g$ is defined as 45° is this study. Note that the switch-to-left or the switch-to-right of the virtual target (*i.e.*, minus or plus $\Delta\theta_g$) is selected randomly. On the way Ⓐ→Ⓑ, $\Delta\theta_g$ is decreased gradually according to equation (8) until a new local minimal is found at location Ⓑ. Again, the location of virtual target switches from A* to B*. Fig. 9 and Fig. 10 show that there is a successive virtual target switching $A^* \rightarrow B_1 \rightarrow B_2 \rightarrow B^*$ when the robot moves around the left upper corner where it is tracked in a trap (to satisfy condition $|\theta_i - \theta_g| > 90°$) three times. After passing through the critical point Ⓑ, the robot keeps approaching the virtual target until reaching the third critical point Ⓒ. Concurrently, the associated orientation of the virtual target is decreased from B* to C. Once more, it takes three times for the robot to escape from the trap situation in the left lower corner on the path Ⓒ→Ⓓ (orientation of the virtual target $C \rightarrow C_1 \rightarrow C_2 \rightarrow C^* \rightarrow D$). Similar navigation procedures take place on the way Ⓓ→Ⓔ (orientation of virtual target $D \rightarrow D_1 \rightarrow D_2 \rightarrow D^* \rightarrow E \rightarrow E^*$). After escaping from the recursive U-shaped trap, the mobile robot revolves in a circle and finally reaches target Ⓣ without any trapping situations (azimuth of virtual target θ_g decreases gradually from E* to T illustrated with a dashed line). The derived trajectory illustrated in Fig. 8 is quite similar to the results derived by Chatterjee and Matsuno (2001). Fig. 10 illustrates the other possible trajectory to escape the same trap situation due to the random choice of the "plus" or "minus" robot-to-target angle $\Delta\theta_g$, as shown in equation (8). Obviously, the mechanism for virtual target switching to the right or to the left (*i.e.*, $\pm\Delta\theta_g$) increases the diversity and possibility of the robot's escaping from the local minima problem.

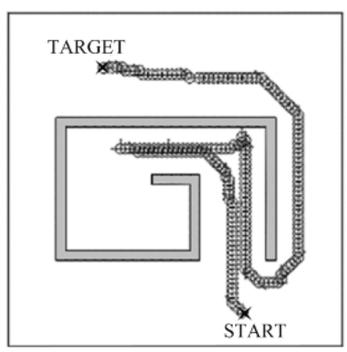

Figure 10. The other possible trajectories to escape the recursive trap situation

4. Motion Planning in Dynamic Environments

4.1 The velocity Obstacle method

This section briefly describes the velocity obstacle (VO) method for the obstacles. For simplicity, the mobile robot and moving obstacles are assumed to be approximated by cylinders and move on a flat floor. Fig. 11(*a*) shows two circular objects *A* and *B* with velocities $\mathbf{v}_A$ and $\mathbf{v}_B$ at time t_0, respectively. Let circle *A* represent the robot and circle *B* represent the obstacle. To compute the VO, obstacle *B* must be mapped into the configuration space of *A*, by reducing *A* to a point $\hat{A}$ and enlarging *B* by the radius of *A* to $\hat{B}$ as Fig. 11(*b*) demonstrates. The Collision Cone, $CC_{A,B}$, is thus defined as the set of colliding relative velocities between $\hat{A}$ and $\hat{B}$:

$$CC_{A,B} = \left\{ \mathbf{v}_{A,B} \mid \lambda_{A,B} \cap \hat{B} \neq \emptyset \right\} \tag{9}$$

where $\mathbf{v}_{A,B} = \mathbf{v}_A - \mathbf{v}_B$ is the relatively velocity of $\hat{A}$ with respect to $\hat{B}$, and $\lambda_{A,B}$ is the line of $\mathbf{v}_{A,B}$.This collision cone is the light gray sector with apex in $\hat{A}$, bounded by the two tangents λ_f and λ_r from $\hat{A}$ to $\hat{B}$ as shown in Fig. 11(*b*). Clearly, any relative velocity $\mathbf{v}_{A,B}$ outside $CC_{A,B}$ is guaranteed to be collision-free, provided that the obstacle $\hat{B}$ maintains its current shape and speed. The collision cone is specific to a particular robot/obstacle pair. To consider situation of multiple obstacles, it is better to establish an equivalent condition on the absolute velocities $\mathbf{v}_A$. This could be done simply by adding the velocity $\mathbf{v}_B$ to each velocity in $CC_{A,B}$, or equivalently, translating the collision cone $CC_{A,B}$ by $\mathbf{v}_B$, as shown in Figure 11(*b*). The velocity obstacle VO (in dark gray sector) is thus defined as:

$$VO = CC_{A,B} \oplus \mathbf{v}_{A,B} \tag{10}$$

where $\oplus$ is the Minkowski vector sum operator. The VO partitions the absolute velocities $\mathbf{v}_A$ into avoiding and colliding velocities. Selecting $\mathbf{v}_A$ outside of VO would avoid collision with B. Velocities $\mathbf{v}_A$ on the boundaries of VO would result in A grazing B.

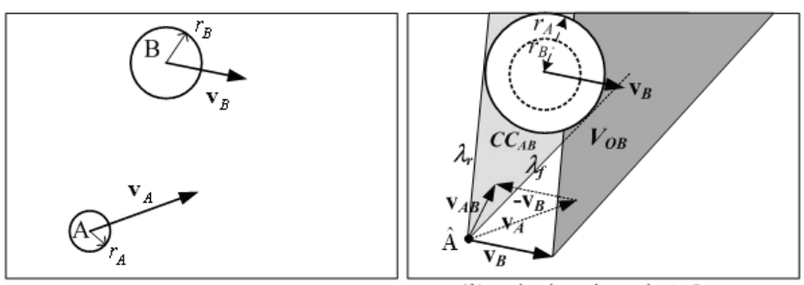

(*a*) two objects on collision course (*b*) velocity obstacle VO

Figure 11. The Velocity Obstacle approach

In the case of multiple obstacles, they are prioritized according to their danger level so that the most imminent collision obstacle is avoided first. In this study, a "collision distance index" is defined as follows to compute the danger level for each obstacle:

$$\delta = \frac{d_{r,obs_j}}{v_j \times T_s}, \quad j = 1,2,\cdots,N_{obs} \tag{11}$$

where d_{r,obs_j} represents the distance between robot and the jth obstacle, v_j is speed of the jth obstacle, and T_s is the sampling time. Obviously, the smaller the collision distance index, the more dangerous to collide obstacle.

4.2 Potential field immune network

A potential field immune network (PFIN) inspired by the biological immune system for robot navigation in dynamic environment is described in this section. For simplicity, one can make the following choices without loss of any generality:

- The mobile robot is an omni-directional vehicle. This means any direction of velocity can be produced at any time. In addition, maximum velocity and acceleration are assumed to be limited considering dynamics of robot and obstacles.

- The mobile robot and moving obstacles under consideration are approximated by cylinder with radius r_r, and r_o. This is not a severe limitation since general polygons can be represented by a collection of circles. Chakravarthy and Ghose (1998) showed that the union of all these circles can still be meaningfully used to predict collision between the irregularly shaped objects. Moreover, the resulting inexact collision cone can still be used effectively for motion planning.
- The mobile robot and moving obstacles move in a flat floor. Moving obstacles may change their velocities (amplitude and direction) at any time.
- The obstacles move along arbitrary trajectories, and that their instantaneous states (position and velocity) are either known or measurable. Prassler *et al.* (2001) have proposed such a sensor system includimg a laser range finder and sonar.

Fig. 12 illustrates the architecture of the proposed potential field immune network. The mechanism, imitating the cooperation between B-T cells, can help the robot adapt to the environment efficiently. In the immunology, the T-cell plays a remarkable key role for distinguishing a "self" from other "non-self" antigens. Resembling the biological immune system, its function is to prioritize the obstacles employing the VO method so that the obstacle with most imminent collision can be identified. In other words, T-cell in PFIN distinguishes an "imminent" from other "far-away" obstacles.

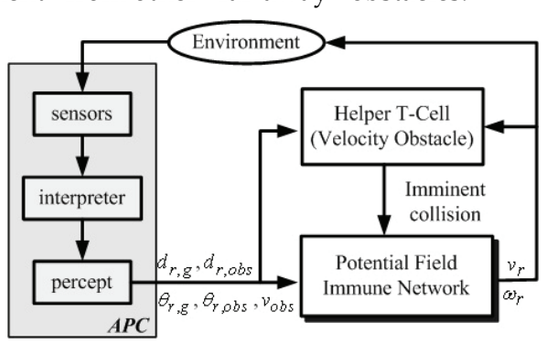

Figure 12. The architecture of the potential field immune network

In PFIN, the antigen's epitope is a situation detected by sensors and provides the information about the relationship between the robot's current states and the obstacles, along with the target as Fig. 12 depicted. Therefore, the antigen represents the local environment surrounding the robot each time interval and its epitopes are a fusion data set for each obstacle as Fig. 13 shows.

$$Ag_j \equiv \{\theta_{r,g}, d_{r,g}, \theta_{r,obs_j}, d_{r,obs_j}\} \qquad j = 1,2,\cdots,N_{obs},$$

where $\theta_{r,g}$ and θ_{r,obs_j} represent the orientations between robot and target, and the jth obstacle, respectively. $d_{r,g}$ and d_{r,obs_j} represent the distance between robot and target, and the jth obstacle, respectively. N_{obs} is the number of moving obstacles.

This scene-based spatial relationship is consistently discriminative between different parts of an environment. The interpreter is regarded as a phagocyte and translates sensor data into perception. The antigen presentation proceeds from the information extraction to the perception translation. An antigen may have several different epitopes, which means that an antigen can be recognized by a number of different antibodies. However, an antibody can bind only one antigen's epitope. In the proposed immune network, the antibody's receptor

is defined as the situation between robot and the imminent collision obstacle as the following

$$Ab_1 \equiv d_{r,g}\ ;\quad Ab_2 \equiv \theta_{r,g}\ ;\quad Ab_3 \equiv d_{r,obs}\ ;\quad Ab_4 \equiv \theta_{r,obs}$$

where $d_{r,obs}$ and $\theta_{r,obs}$ represent the distance and orientation between robot and the imminent collision obstacle, respectively.

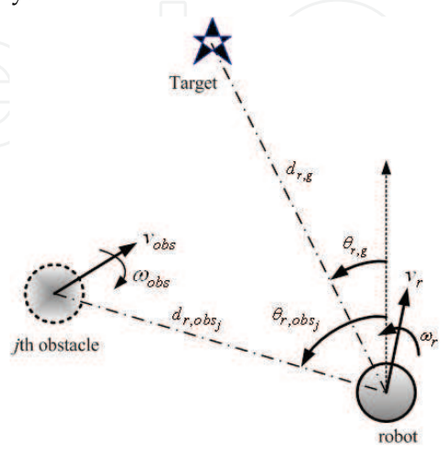

Figure 13. Configuration of mobile robot and its relatives to target and obstacles

The response of the overall immune network is thus derived by determining the set of affinities associated with the receptors and the structural similarity between antigen and antibody defined by quantification of the distance in antigen space. In this study, the collective immune response function of the immune network is defined as the following immune functions,

$$\begin{cases} v_r = f(Ab_1) + f(Ab_3) \\ \omega_r = f(Ab_2) + f(Ab_4) \end{cases} \tag{12}$$

where v_r and ω_r are the robot's velocity and angular velocity outputs, respectively. This is a kind of artificial potential field approach since it considers a virtual attractive force between the robot and the target (*i.e.* $f(Ab_1)$ and $f(Ab_2)$) as well as virtual repulsive forces between the robot and the obstacle (*i.e.* $f(Ab_3)$ and $f(Ab_4)$). The resultant force on the robot is then used to decide the velocities (*i.e.* v_r and ω_r) of its movements. Functions $f(Ab_i)$ are expressed as following,

$$f(Ab_i) = K_i \times \frac{\sum_{j=1}^{4} m_i \times m_{ij}}{\sum_{j=1}^{4} m_{ij}}, \quad i = 1, 2, 3, 4$$

where m_i is the affinity of antigen (the most imminent collision obstacle) and the ith antibody, m_{ij} is the stimulation/suppressive affinity between the ith and jth antibody. Corresponding constant parameters are K_1= 20, K_2= 30, K_3= 15, K_4= 30, respectively. Note that these values are defined according to the velocity limitation of the robot and obstacles. The affinity of the antigen and the ith antibody m_i is fuzzified using the fuzzy set definitions as Fig. 14 illustrates.

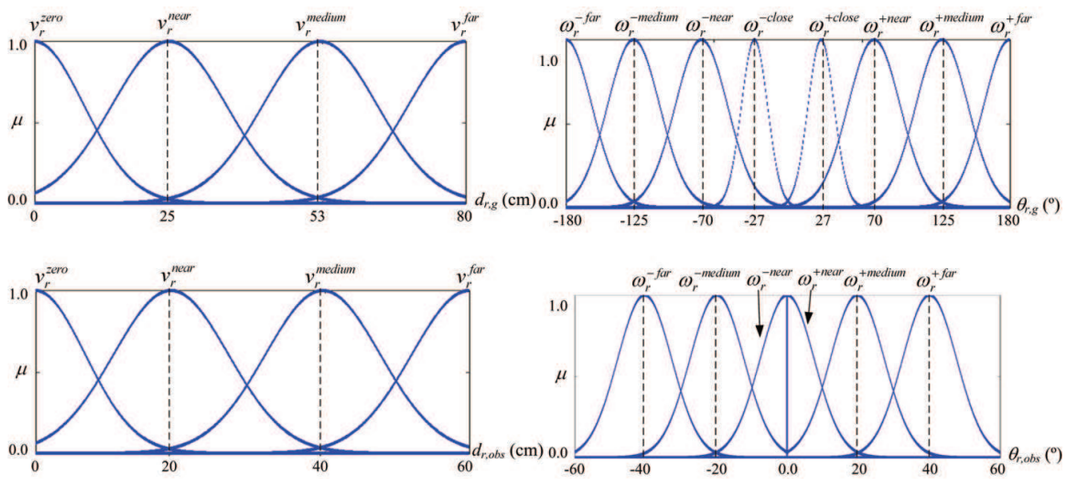

Figure 14. Membership functions of antibodies

The mapping from the fuzzy subspace to the TSK model is represented as fuzzy if-then rules in the form of

IF $d_{r,g}$	is	*zero*	THEN	v_r = 0cm/s
IF $d_{r,g}$	is	*near*	THEN	v_r = 10cm/s
IF $d_{r,g}$	is	*medium*	THEN	v_r = 15cm/s
IF $d_{r,g}$	is	*far*	THEN	v_r = 20cm/s
IF $\theta_{r,g}$	is	*-far*	THEN	ω_r = -30°/s
IF $\theta_{r,g}$	is	*-medium*	THEN	ω_r = -25°/s
IF $\theta_{r,g}$	is	*-near*	THEN	ω_r = -20°/s
IF $\theta_{r,g}$	is	*-close*	THEN	ω_r = -10°/s
IF $\theta_{r,g}$	is	*+close*	THEN	ω_r = 10°/s
IF $\theta_{r,g}$	is	*+near*	THEN	ω_r = 20°/s
IF $\theta_{r,g}$	is	*+medium*	THEN	ω_r = 25°/s
IF $\theta_{r,g}$	is	*+far*	THEN	ω_r = 30 °/s
IF $d_{r,obs}$	is	*zero*	THEN	v_r = -15cm/s
IF $d_{r,obs}$	is	*near*	THEN	v_r = -10cm/s
IF $d_{r,obs}$	is	*medium*	THEN	v_r = -5cm/s
IF $d_{r,obs}$	is	*far*	THEN	v_r = 0cm/s
IF $\theta_{r,obs}$	is	*-far*	THEN	ω_r = 10°/s
IF $\theta_{r,obs}$	is	*-medium*	THEN	ω_r = 20°/s
IF $\theta_{r,obs}$	is	*-near*	THEN	ω_r = 30°/s
IF $\theta_{r,obs}$	is	*+near*	THEN	ω_r = -30°/s
IF $\theta_{r,obs}$	is	*+medium*	THEN	ω_r = -20°/s
IF $\theta_{r,obs}$	is	*+far*	THEN	ω_r = -10°/s

Consequently, the centroid defuzzification method is employed to calculate the weighted average of a fuzzy set,

$$m_i = \frac{\sum_{k=0}^{L} \mu_k y_k}{\sum_{k=0}^{L} \mu_k}, \quad i = 1, 2, 3, 4 \tag{13}$$

where μ_k represent the matching degree of the kth rule and y_k represent its corresponding output value. Finally, the stimulation and suppressive interaction m_{ij} between the ith and jth antibodies are optimized utilizing genetic algorithms. Hundreds of different circumstances with randomly generated moving obstacles were employed to optimize the affinity values m_{ij} of PFIN. Fig. 15 demonstrates one of the cases in which several tens of obstacles circumrotate at randomly generated positions with different radius. Fig. 15(*a*) shows that robot reaches target successfully while Fig. 15(*b*) demonstrates that robot is failed to reach target in the optimization procedure. Table 1 lists the derived optimal stimulation and suppressive affinity value m_{ij} between the ith and jth antibodies.

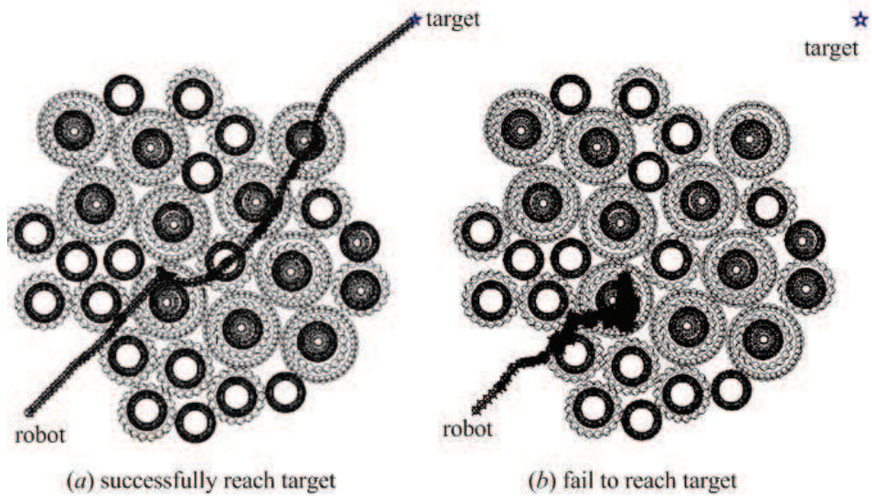

Figure 15. Randomly generated moving obstacles for optimizing m_{ij}

m_{ij}	j=1	j=2	j=3	j=4
i=1	**1**	**-0.13**	**-0.24**	**-0.04**
i=2	**-0.02**	**1**	**-0.11**	**-0.42**
i=3	**-0.37**	**-0.84**	**1**	**0.92**
i=4	**-0.21**	**-0.92**	**-0.31**	**1**

Table 1. The stimulation and suppressive interaction affinity value m_{ij}

5. Simulation and discussions

5.1 Motion Planning in Stationary Environments

Numerous simulation examples presented by researchers (Xu, 2000; Chatterjee & Matsuno, 2001; Kubota et al., 2001) were conducted to demonstrate the performance of mobile robot navigation employing RIN to various unknown environments; in particular, the capability of escaping from the traps or the wandering situations described. Assuming that the robot has eight uniformly distributed distance sensors (*i.e.* N_s=8) and eight moving directions including forward, left, right, back, forward left, forward right, back left, and back right (*i.e.* N_{Ab}=8) as Fig. 16 shows. Fig. 17(*a*) demonstrates the similar trajectory of the mobile robot to escape from loop-type and dead-end-type trapping situations in (Chatterjee & Matsuno, 2001). Again, Fig. 17(*b*) demonstrates the other possible trajectory (escaping from the left side) due to the random selection scheme ("±") mentioned previously.

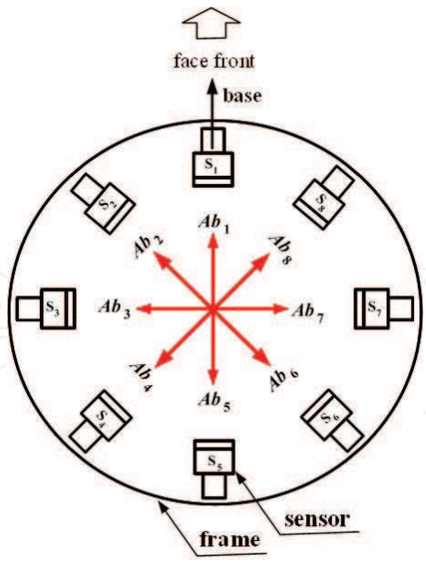

Figure 16. Configuration of mobile robot employed in simulation

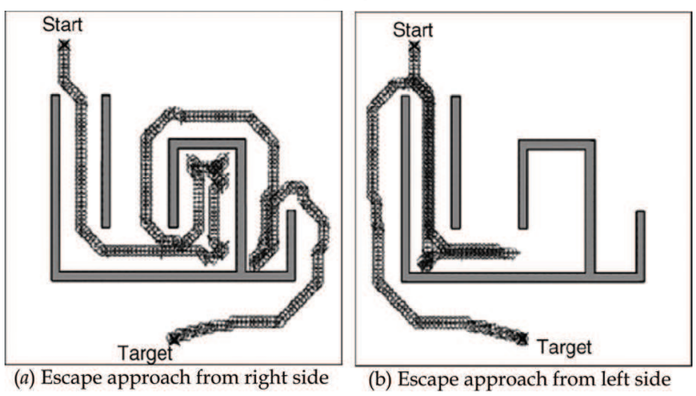

(a) Escape approach from right side (b) Escape approach from left side

Figure 17. Robot trajectories to escape from loop type and dead-end type trap situation

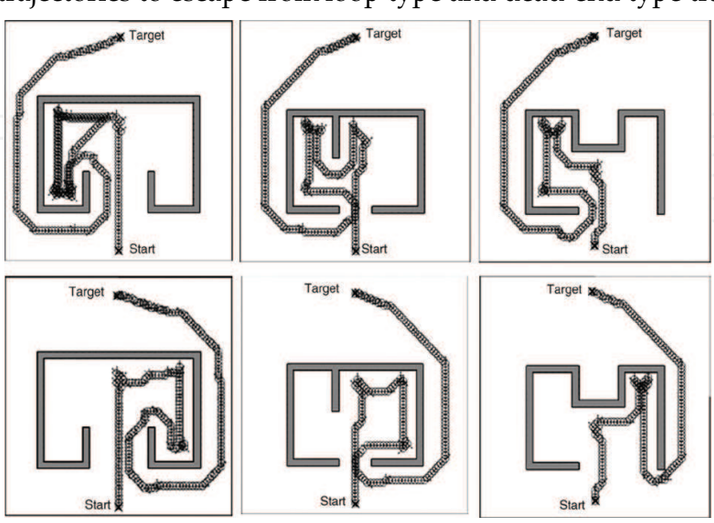

Figure 18. Robot trajectories to escape from different trapping situations

To validate the efficiency of the proposed scheme further, three trap environments adopted in (Madlhava & Kalra, 2001) were utilized in this study. Obviously, the simulation results depicted in Fig. 18 show that the robot is capable of escaping from all the traps as expected. Finally, the most famous and utilized example, U-shaped trap problem, is employed in this study. Fig. 19 shows part of the paths of the robot escaping from the U-shaped trap with different L/W (length/width) ratios. Clearly, the robot is capable of escaping from different ratio U-shaped environments. As to the double U-shaped trap environment (Kunota et al., 2001), Fig. 20 demonstrates the four trajectories for the robot to escape utilized RIN. Apparently, RIN successfully drives the robot to escape the double U-shaped trap.

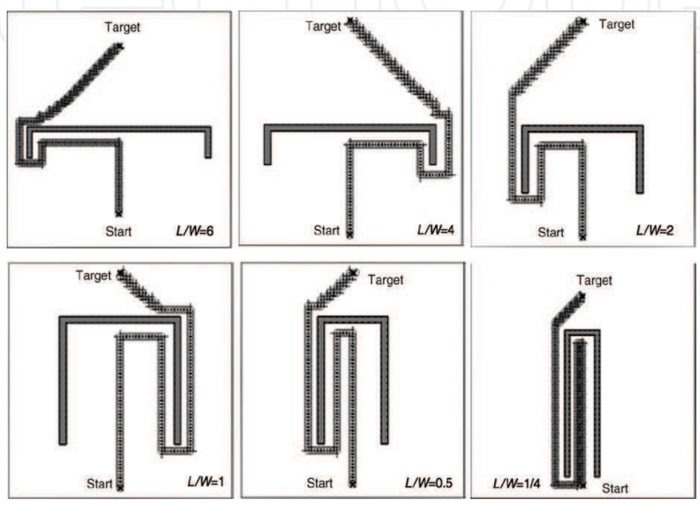

Figure 19. Robot trajectories to escape from U-shaped trap with different length/width ratio

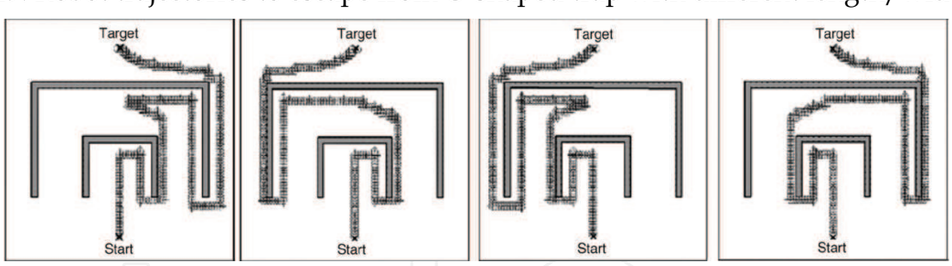

Figure 20. Robot trajectories to escape from double U-shaped trap

5.2 Motion Planning in Dynamic Environments

Numerous simulations have been utilized to evaluate the performance and effectiveness of a mobile robot among multiple moving obstacles using the proposed PFIN. In the simulations, the size of the test field is 5m ×5m, and the radius of robot and obstacles are r_r = 0.1 m and r_o = 0.1 m, respectively. In addition, the speed constraints on mobile robot and moving obstacles are $v_{r\ \max}$ = 20 cm/s, $v_{o\ \max}$ = 20 and $\omega_{r\ \max}$ = 30°/s. The sampling time for each step is T_s = 0.03sec. To carry out these computations, a computer program was developed employing C++ programming tools with a graphical user interface. The simulation examples demonstrated in figures are given with graphical representations in which the trajectories of the moving object and the robot are described. Moreover, figures show the velocity-time history and azimuth-time history of the robot, respectively. In each figure, circles indicate the position of the robot and obstacles at each time instant when the robot executed an action. A high concentration of

circles indicates a lower velocity (of the obstacle and of the robot) whilst a low concentration is a reflection of a greater velocity. In addition, the state responses (speed and orientation) of robot and obstacles are depicted in the figures. Obviously, the robot smoothly avoids the moving obstacles and reaches goal as expected for all cases.

Fig. 21 reveals that an obstacle coming from left side along a straight line cross the robot path. Within the interval of points A and D (at fifth and fourteenth sampling instant respectively), the obstacle slows down its speed in front of the robot's way to goal. Obviously, the robot appears a "hunting" behavior in this duration. Figs. 22(*a*)-22(*d*) explain this behavior employing the VO concept. At position A as Fig. 22(*a*) shown, the robot will collide with the obstacle since the relative velocity between robot and obstacle (*i.e.* $\mathbf{v}_{ro}$) is inside the velocity cone CC_{AB}. Thus the robot turns left (positive angular velocity as Fig. 21 shown) to avoid collision and reach position B. Because $\mathbf{v}_{ro}$ is outside the velocity cone in position B and there is no danger to collide the obstacle as Fig. 22(*b*) depicted, the robot turns right again due to the attraction force from the target. Once more, robot turns left to avoid collision at position C as Fig. 22(*c*) demonstrated. The "hunting" behavior (*i.e.* turn left and then turn right) is repeated until the robot reaches the position D. Subsequently, the robot finds that it may collide with the obstacle in next time step again as Fig. 22(*d*) shown. Robot decelerates its speed to stop quickly and then goes back to the position E (negative velocity from position D to E as Fig. 21 shown). Finally, the robot turns right and passed over behind the obstacle rapidly to reach the goal since the obstacle is no longer a threat.

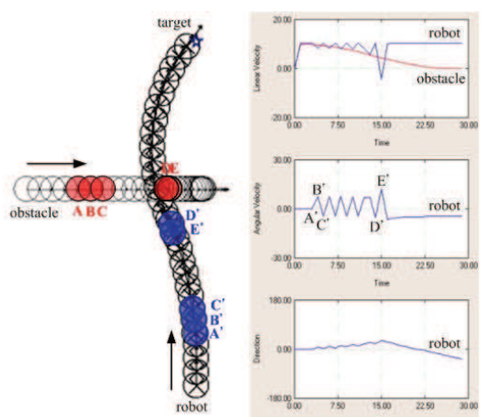

Figure 21. Trajectories and associated state responses of mobile robot and obstacle

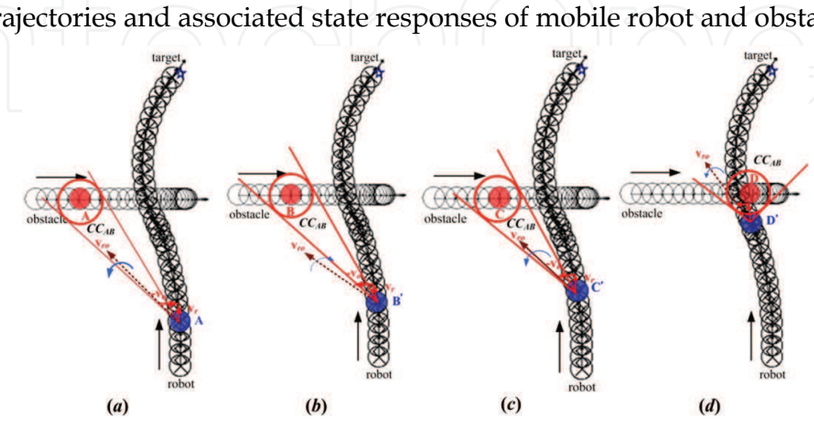

Figure 22. Velocity cone of robot at different positions

Fig. 23 shows a simulation result by which the robot can avoid two moving obstacles one after another then reach the goal. These obstacles come from different sides with arbitrary trajectory and varying speed cross the robot path. Similar to the previous simulation, the robot decelerates its speed at points A and B to avoid the first and second obstacles separately. Then it accelerates and moves towards the goal without collision

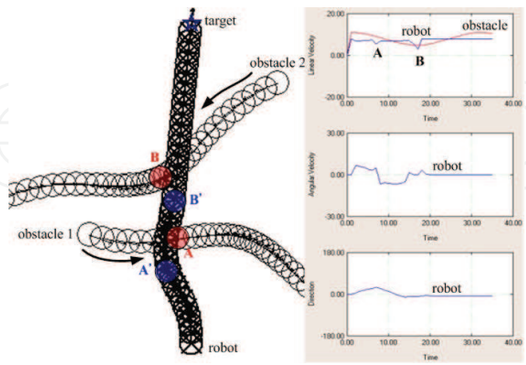

Figure 23. Trajectories and associated state responses of mobile robot and obstacles

Fig. 24 demonstrates the motion planning of a mobile robot tracking a moving goal while avoiding two moving obstacles. Obviously, mobile robot is able to reach goal and avoid moving obstacles no matter what the goal is fixed or moving employing the proposed PFIN. The robot decelerates at position A′ to wait for the first obstacle while accelerates at position C′ to exceed the second obstacle. Moreover, robot turns bigger angles at position B′ to follow the moving target compared with that of fixed target case. Note that the two obstacles have the same trajectories in both cases.

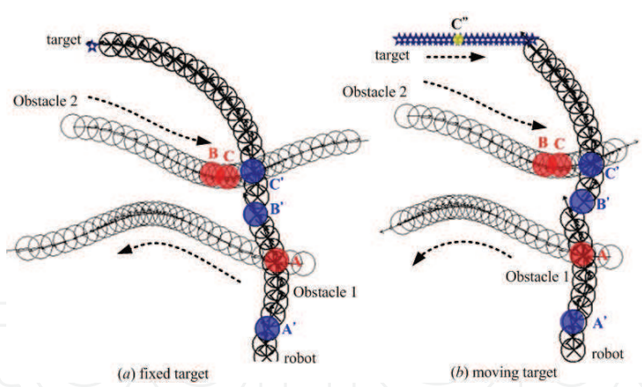

Figure 24. Trajectories of robot and obstacles for fixed/moving goals

Fig. 25 demonstrates another example of motion planning for the case of suddenly moving/stopped obstacle. Figs. 25(*a*)-25(*d*) illustrate a simulation result by which the robot successfully avoid two moving and two static obstacles. As usual, the robot exceeds the first moving obstacle at position A′ and waits for the second moving obstacle at position C′. Fig. 25(*e*) demonstrates that the robot reaches target safely even though the second static obstacle abruptly moves when the robot approaches it. Fig. 25(*f*) shows the similar result except that the second moving obstacle unexpectedly stops when it near the robot. Note that both the moving and stopping actions of the second static obstacle shown in Fig. 25(*e*) and Fig. 25(*f*) are pre-programmed to test the performance of the proposed architecture.

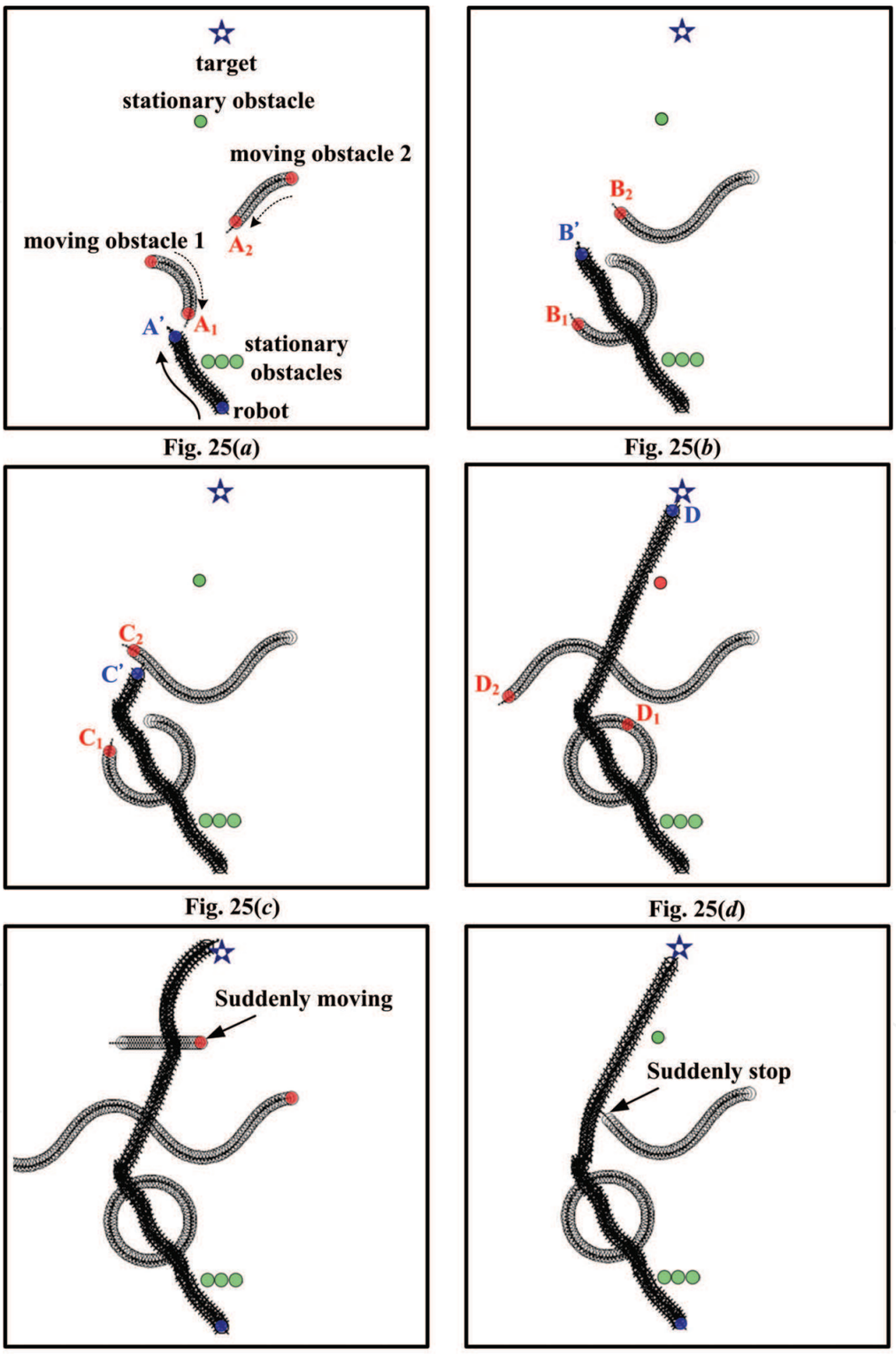

Figure 25. Trajectories of robot and obstacles for suddenly moving/stopped obstacle

6. Experimental Results

Numerous experiments were implemented to evaluate the performance in real application. Fig. 26 shows the mobile robot (with omni-directional wheel) used. Its dimension is 416mm×363.7mm×670mm. The robot installed with 8 ultrasonic sensors, two web-cams, and a laser range finder. Figs.27, 28 demonstrate the pictures of the robot navigate in two "U" shape obstacles (with different length and width: 160mm×320mm, and 300mm×100mm) and their corresponding trajectories, respectively.

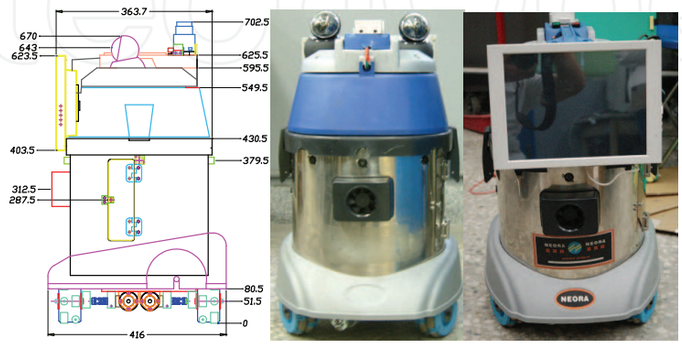

Figure 26. Dimension and pictures of the mobile robot

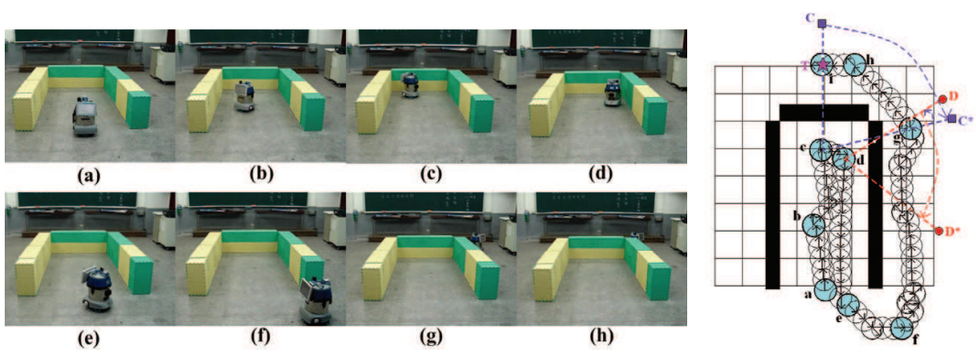

Figure 27. Navigation of robot in 160mm×320mm "U" obstacle and corresponding trajectories

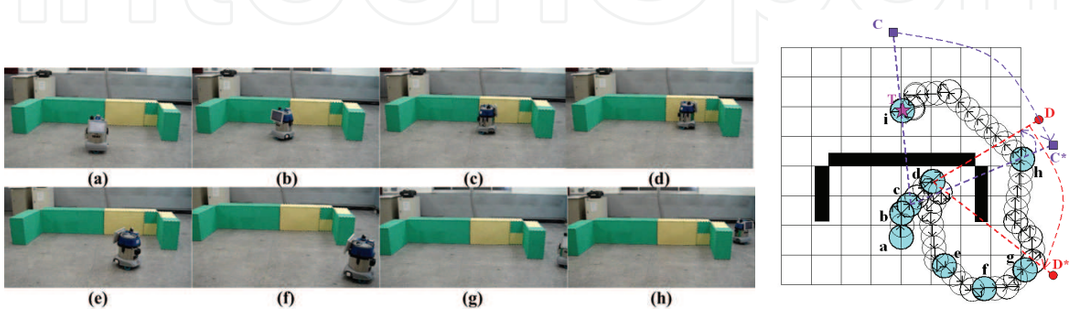

Figure 28. Navigation of robot in 300mm×100mm "U" obstacle and corresponding trajectories

Fig. 29 illustrate the pictures of the robot navigate in a "sequential-U" shape obstacle (400*mm*×190*mm* with a 90*mm* bar in middle) and its corresponding trajectory, respectively.

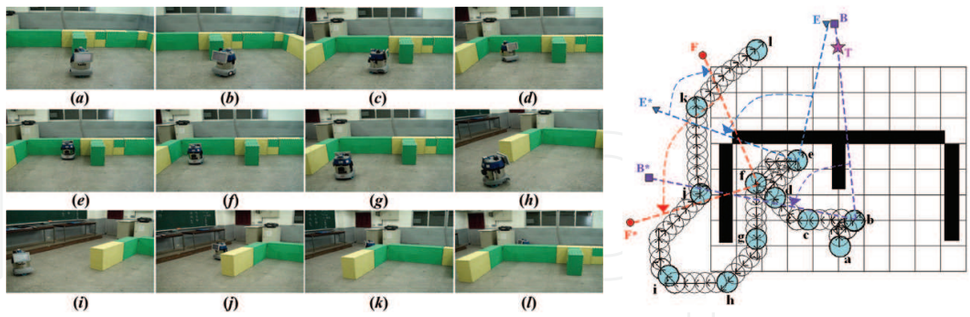

Figure 29. Trajectories in "sequential-U" shape obstacle and corresponding trajectories

All these figures show that the mobile robot is capable of navigating to the goal and escaping from local minimum traps employing the proposed reactive immune network. Note that mobile robot can approach target from both sides randomly as described in previous section.

6. Conclusion

Two different kind of reactive immune networks inspired by the biological immune system for robot motion planning are constructed in this study. The first one is a potential filed based immune network with an adaptive virtual target mechanism to solve the local minima problem navigating in stationary environments. Simulation and experimental results show that the mobile robot is capable of avoiding stationary obstacles, escaping traps, and reaching the goal efficiently and effectively. Employing the Velocity Obstacle method to determine the imminent collision obstacle, the second architecture guide the robot avoiding collision with the most danger object (moving obstacle) at every time instant. Simulation results are presented to verify the effectiveness of the proposed architecture in dynamic environment. Currently, laser range finder is utilizing to evaluate the performance of the proposed mechanism.

7. Acknowledgements

The authors would like to acknowledge the National Science Council, Taiwan, R.O.C., for making this work possible with grants NSC 95-2221-E-036-009 and NSC 96-2221-E-036-032-MY2.

8. References

Baraquand, J.; & Latombe, J.C. (1990). A Monte-Carlo algorithm for path planning with many degrees of freedom, *Proceedings of the IEEE International Conference on Robotics and Automation*, pp. 1712-1717, Cincinnati, OH, May, 1990

Carneiro, J.; Coutinho, A.; Faro, J. & Stewart, J. (1996). A model of the immune network with B-T cell co-operation I-prototypical structures and dynamics, *Journal of theoretical Biological*, Vol.182, No.4, 1996, pp. 513-529

Chakravarthy, A. & Ghose, D. (1998). Obstacle Avoidance in a Dynamic Environment: A Collision Cone Approach, *IEEE Transactions on Systems, Man, and Cybernetics – Part A: Systems and Humans*, Vol.25, No.5, 1998, pp. 562-574

Chatterjee, R. & Matsuno, F. (2001). Use of single side reflex for autonomous navigation of mobile robots in unknown environments, *Robotics and Autonomous Systems*, Vol.35, No.2, 2001, pp. 77-96

Chang, H. (1996). A new technique to handle local minima for imperfect potential field based motion planning, *Proceedings of the IEEE International Conference on Robotics and Automation*, pp. 108-112, Minneapolis, Minnesota, April, 1994

Dasgupta, D. (1997). Artificial neural networks and artificial immune systems: similarities and differences, *IEEE International Conference on Systems, Man, and Cybernetics*, pp. 873-878, Orlando, Florida, October, 1997

Dasgupta, D. (1999). *Artificial Immune Systems and Their Applications*, Springer-Verlag, ISBN 3-540-64390-7, Berlin Heidelberg

de Castro, L.N. & Jonathan, T. (1999). *Artificial immune systems: A new Computational Intelligence Approach*, Springer-Verlag, ISBN 1-85233-594-7, London

Duan, Q.J.; Wang, R.X.; Feng, H.S. & Wang, L.G. (2004). An immunity algorithm for path planning of the autonomous mobile robot, *IEEE 8th International Multitopic Conference*, pp. 69-73, Lahore, Pakistan, December, 2004

Duan, Q.J.; Wang, R.X.; Feng, H.S. & Wang, L.G. (2005). Applying synthesized immune networks hypothesis to mobile robots, *IEEE International Conference on Autonomous Decentralized Systems*, pp. 69-73, Chengdu, China, April, 2005

Farmer, J.D.; Packard, N.H. & Perelson, A.S. (1986). The immune system adaptation, and machine learning, *Physica*, Vol.22-D, Vol.2, No.1-3, 1986, pp. 187-204

Ferrari, C.; Pagello, E.; Ota, J.; & Arai, T. (1998). Multi-robot motion coordination in space and time, *Robotics and Autonomous Systems*, Vol.25, No.2, 1998, pp. 219-229

Fiorini, P. & Shiller, Z. (1998). Motion planning in dynamic environments using velocity obstacles, *International Journal of Robotics Research*, Vol.17, No.7, 1998, pp. 760-772

Fujimura, K. & Samet, H. (1989). A hierarchical strategy for path planning among moving obstacles, *IEEE Trans on Robot and Automat*, Vol.5, No.1, 1989, pp. 61-69

Fujimori, A. (2005). Navigation of mobile robots with collision avoidance for moving obstacles, *Proc Instn Mech Engrs Part I: J Systems and Control Engineering*, Vol.219, No.1, 2005, pp. 99-110

Ge, S. S. & Cui, Y. J. (1989). Dynamic motion planning for mobile robots using potential field method, *Autonomous Robots*, Vol.13, No.3, 1989, pp. 207–222

Hart, E.; Ross, P.; Webb, A. & Lawson, A. (2003). A role for immunology in "next generation" robot controllers, *Lecture Notes in Computer Science*, Vol.2787, 2003, pp. 46-56

Hightower, R.; Forrest, S. & Perelson, A. S. (1995). The evolution of emergent organization in immune system gene libraries, *Proceedings of Sixth International Conference on Genetic Algorithms*, pp. 344-350, Pittsburgh, PA, July, 1995

Hoffmann, G.W. (1989). The immune system: a neglected challenge for network theorists, *IEEE International Symposium on Circuits and Systems*, pp. 1620-1623, Portland, OR, May, 1989

Ishida, Y. (1997). The immune system as a prototype of autonomous decentralized systems: an overview, *Proceedings of Third International Symposium on autonomous decentralized systems*, pp. 85-92, Berlin, Germany, April, 1997

Ishiguro, A.; Watanabe, Y. & Uchikawa, Y. (1995). An immunological approach to dynamic behavior control for autonomous mobile robots, *IEEE/RSJ International Conference on Intelligent Robots and Systems*, pp. 495-500, Pittsburg, PA, 1995

Jerne, N.K. (1973). The immune system, *Scientific American*, Vol.229, No.1, 1973, pp. 52-60

Kondo, A. T.; Watanabe, Y.; Shirai, Y. & Uchikawa, Y. (1997). Emergent construction of artificial immune networks for autonomous mobile robots, *IEEE International Conference on Systems, Man, and Cybernetics*, pp. 1222-1228, Orlando, Florida, October, 1997

Kubota, N.; Morioka, T.; Kojima, F. & Fukuda, T. (2001). Learning of mobile robots using perception-based genetic algorithm, *Measurement*, Vol.29, No.3, 2001, pp. 237-248

Lee, D.-W. & Sim, K.-B. (1997). Artificial immune network-based cooperative control in collective autonomous mobile robots, *IEEE International Workshop on Robot and Human Communication*, pp. 58-63, Sendai, Japan, September, 1997

Lee, D.-J.; Lee, M.-J.; Choi, Y.-K. & Kim, S. (2000). Design of autonomous mobile robot action selector based on a learning artificial immune network structure, *Proceedings of the fifth Symposium on Artificial Life and Robotics*, pp. 116-119, Oita, Japan, January, 2000

Lee, S.; Adams, T.M. & Ryoo, B.-Y. (1997). A fuzzy navigation system for mobile construction robots, *Automation in Construction*, Vol.6, No.2, 1997, pp. 97-107

Liu, C.; Marcelo Jr., H.A.; Hariharan, K. & Lim, S.Y. (2000). Virtual obstacle concept for local-minimum-recovery in potential-field based navigation, *Proceedings of the IEEE International Conference on Robotics and Automation,* pp. 983-988, San Francisco, CA, April 2000

Luh, G.-C. & Cheng, W.-C. (2002). Behavior-based intelligent mobile robot using immunized reinforcement adaptive learning mechanism, *Advanced Engineering Informatics*, Vol.16, No.2, 2002, pp. 85-98

Madlhava, K. & Kalra, P.K. (2001). Perception and remembrance of the environment during real time navigation of a mobile robot, *Robotics and Autonomous Systems*, Vol.37, No.1, 2001, pp. 25-51

Mucientes, M.; Iglesias, R.; Regueiro, C. V.; Bugarín, A.; Cariñena, P. & Barro, S. (2001). Fuzzy temporal rules for mobile robot guidance in dynamic environments, *IEEE Transactions on Systems, Man, and Cybernetics – Part C: Applications and Reviews*, Vol.21, No.3, 2001, pp. 391-398

Oprea, M.L. (1996). *Antibody repertories and pathogen recognition: the role of germline diversity and somatic hypermutation*, PhD Dissertation, Department of Computer Science, The University of New Mexico, Albuquerque, New Mexico

Prassler, E.; Scholz, J. & Fiorni, P. (2001). A robotic wheelchair for crowded public environments, *IEEE Robotics and Automation Magazine*, Vol.7, No.1, 2001, pp. 38-45

Qu, Z.; Wang, J. & Plaisted, C.E. (2004). A new analytical solution to mobile robot trajectory generation in the presence of moving obstacles, *IEEE Transactions on Robotics*, Vol.20, No.6, 2004, pp. 978-993

Roitt, I.; Brostoff, J. & Male, D.K. (1998). *Immunology*, Mosby-Harcourt Publishers Ltd, ISBN 0723429189, London

Timmis, J.; Neal, M. & Hunt, J. (1999). Data analysis using artificial immune systems, cluster analysis and Kohonen networks: some comparisons, *IEEE International Conference on Systems, Man, and Cybernetics,* pp. 922-927, Tokyo, Japan, October, 1999

Vargas, P.A.; de Castro, L.N.; Michelan, R. & Von Zuben, F.J. (2003). Implementation of an Immuno-Gentic Network on a Real Khepera II Robot, *IEEE Congress on Evolutionary Computation*, pp. 420-426, Canberra, Australia, December, 2003

Xu, W.L. (2000). A virtual target approach for resolving the limit cycle problem in navigation of a fuzzy behaviour-based mobile robot, *Robotics and Autonomous Systems*, Vol.30, No.4, 2000, pp. 315-324

Yun, X. & Tan, K.-C. (1997). A wall-following method for escaping local minima in potential field based motion planning, *Proceedings of the IEEE International Conference on Advanced Robotics*, pp. 421-426, Monterey, CA, July, 1997

Motion Planning

Edited by Xing-Jian Jing

ISBN 978-953-7619-01-5
Hard cover, 598 pages
Publisher InTech
Published online 01, June, 2008
Published in print edition June, 2008

In this book, new results or developments from different research backgrounds and application fields are put together to provide a wide and useful viewpoint on these headed research problems mentioned above, focused on the motion planning problem of mobile ro-bots. These results cover a large range of the problems that are frequently encountered in the motion planning of mobile robots both in theoretical methods and practical applications including obstacle avoidance methods, navigation and localization techniques, environmental modelling or map building methods, and vision signal processing etc. Different methods such as potential fields, reactive behaviours, neural-fuzzy based methods, motion control methods and so on are studied. Through this book and its references, the reader will definitely be able to get a thorough overview on the current research results for this specific topic in robotics. The book is intended for the readers who are interested and active in the field of robotics and especially for those who want to study and develop their own methods in motion/path planning or control for an intelligent robotic system.

How to reference

In order to correctly reference this scholarly work, feel free to copy and paste the following:

Guan-Chun Luh and Wei-Wen Liu (2008). An Immunological Approach to Mobile Robot Navigation, Motion Planning, Xing-Jian Jing (Ed.), ISBN: 978-953-7619-01-5, InTech, Available from: http://www.intechopen.com/books/motion_planning/an_immunological_approach_to_mobile_robot_navigation

INTECH
open science | open minds

InTech Europe
University Campus STeP Ri
Slavka Krautzeka 83/A
51000 Rijeka, Croatia
Phone: +385 (51) 770 447
Fax: +385 (51) 686 166
www.intechopen.com

InTech China
Unit 405, Office Block, Hotel Equatorial Shanghai
No.65, Yan An Road (West), Shanghai, 200040, China
中国上海市延安西路65号上海国际贵都大饭店办公楼405单元
Phone: +86-21-62489820
Fax: +86-21-62489821

© 2008 The Author(s). Licensee IntechOpen. This chapter is distributed under the terms of the Creative Commons Attribution-NonCommercial-ShareAlike-3.0 License, which permits use, distribution and reproduction for non-commercial purposes, provided the original is properly cited and derivative works building on this content are distributed under the same license.